

## Primary instabilities in Faraday waves under an arbitrarily periodic excitation

Chen Weizhong\* and Wei Rongjue

*Institute of Acoustics and State Key Laboratory of Modern Acoustics, Nanjing University, Nanjing 210093, People's Republic of China*

(Received 15 July 1997)

Under a vertically arbitrarily periodic excitation, the primary Faraday instability of the flat surface of a viscous fluid layer has been analyzed by the linear stability theory. As an application, the pattern instabilities induced by the two-frequency forcing have been calculated numerically according to the known experiments. The theoretical marginal instability curves as well as the bicriticality threshold curves are in good agreement with those measured in recent experiments. [S1063-651X(98)09403-3]

PACS number(s): 47.20.Dr, 47.20.Gv, 47.35.+i, 47.54.+r

### I. INTRODUCTION

The experimental observation of standing waves on the surface of a fluid layer subject to a vertical vibration dates back to Faraday [1]. When the forcing amplitude exceeds a critical value, the plane surface undergoes a primary instability to a standing-wave pattern [1–6] or a solitary wave [7,8]. A second instability to the transverse wave amplitude modulation [9] or a state of spatiotemporal chaos [9,10] will arise at a larger forcing amplitude. Depending on the parameters of the fluid and the excitation, spatially periodic patterns in the forms of lines, squares, and hexagons have been observed in large-aspect-ratio containers [1–6]. Usually the vertical excitation is in the form of the single-frequency sinusoidal wave [1–4,7,8] as Faraday used. On the theoretical front, Benjamin and Ursell's investigation of the linear stability [11] analyzed the Faraday waves in an ideal fluid layer excited sinusoidally and showed that the fluid dynamic equations could be reduced to a system of Mathieu equations which allowed the harmonic as well as the subharmonic response. Kumar and Tuckerman presented a matrix method for analyzing Faraday instabilities of a shallow layer of viscous fluids [12,13]. In this approach, one can easily determine the parameter region for both harmonic and subharmonic responses by an approximate truncation of the order of the matrix in infinite order. Although this method is quite successful (e.g., a prediction [12] that there would be a harmonic onset pattern rather than a subharmonic one usually if the wavelength became comparable to the height of the layer has been confirmed by a recent experiment [14]), it is only suitable for the primary Faraday instability under a single-frequency excitation. However, Müller [5] has observed patterns in both harmonic and subharmonic responses with respect to the fundamental frequency under excitation of two commensurable frequencies. Furthermore, a systematic experiment on patterns induced by the two-frequency excitation has also been carried out by Edwards and Fauve [6]. They observed patterns in the forms of lines and hexagons and a 12-fold quasipattern that has long-range order but no spatial periodicity. In this paper we will extend Kumar's approach to the case under an arbitrarily periodic excitation and

make possible the prediction of the marginal instability curve (MIC) separating the patterns and flat surface and the bicriticality threshold curve (BTC) separating the onset patterns of the harmonic and subharmonic responses under any periodic excitation. As applications we will analyze and explain the BTCs [5] and MICs [6] in Faraday experiments under two-frequency excitations.

### II. LINEAR INSTABILITY UNDER AN ARBITRARILY PERIODIC EXCITATION

We consider a plate with a fluid layer of height  $h$  and velocity  $\mathbf{u}(x,y,z,t) \equiv \{u,v,w\}(x,y,z,t)$ . The vertical axis is  $z$  and the free surface is initially flat, stationary, and coincident with the  $z=0$  plane by choice of a coordinate system. The plate located on  $z=-h$  is excited vertically by an arbitrary time function with the period  $2\pi/\omega$ ,

$$a(t) = \sum_{j=1}^N a_j \cos(j\omega t + \phi_j), \quad (1)$$

where  $\omega/2\pi$  is the fundamental frequency,  $a_j$  and  $\phi_j$  ( $j=1, \dots, N$ ) are acceleration amplitudes and phases of components, and  $N$  is an arbitrary integer. The excitation is equivalent to a temporally modulated gravitational acceleration

$$g(t) = \sum_{j=-N}^N g_j e^{ij\omega t}, \quad (2)$$

where

$$g_0 = g, \quad g_j = -\frac{1}{2} a_j e^{i\phi_j}, \quad g_{-j} = g_j^* \quad (j=1, \dots, N), \quad (3)$$

with  $g$  being gravity acceleration and the asterisk standing for a complex conjugate. As soon as the instability sets in, the free surface becomes  $z = \xi(x,y,t)$ . For an incompressible fluid with uniform density  $\rho$  and kinetic viscosity  $\nu$ , we can reduce the linearized hydrodynamic equations for the perturbation fields  $\mathbf{u}(x,y,z,t)$  and  $\xi(x,y,t)$  into a linear instability problem [12]

\*Electronic address: wzchen@nju.edu.cn

$$[\partial_t - \nu(\partial_{zz} - k^2)](\partial_{zz} - k^2)w = 0, \quad (4)$$

$$(\partial_{zz} + k^2)w|_{z=0} = 0, \quad (5)$$

$$w|_{z=-h} = 0, \quad (6)$$

$$\partial_z w|_{z=-h} = 0, \quad (7)$$

$$(\partial_t - \nu\partial_{zz} + 3\nu k^2)|_{z=0} = -\left(g(t) + \frac{\sigma}{\rho}k^2\right)k^2\xi, \quad (8)$$

$$\partial_t \xi = w|_{z=0}, \quad (9)$$

where real functions  $w = w(z, t)$  and  $\xi = \xi(t)$  are defined as  $w(x, y, z) = w(z) \sin(k_x x + k_y y)$  and  $\xi(x, y, t) = \xi(t) \sin(k_x x + k_y y)$  and  $k_x$  and  $k_y$  satisfy  $k^2 = k_x^2 + k_y^2$  with the horizontal wave number  $k$ , respectively. Here  $g(t)$  is in the form of an arbitrary multiple-frequency function of time  $t$  instead of the single-frequency one [12,13]. The solutions to Eqs. (4)–(9) can be assumed to be of Floquet form because the time-modulation gravitational acceleration  $g(t)$  in Eq. (2) is still a periodic function of time  $t$  with period  $2\pi/\omega$ ,

$$\xi(t) = e^{(s+i\alpha\omega)t} \sum_{n=-\infty}^{\infty} \xi_n e^{in\omega t}, \quad (10)$$

$$w(z, t) = e^{(s+i\alpha\omega)t} \sum_{n=-\infty}^{\infty} w_n(z) e^{in\omega t}, \quad (11)$$

where  $s+i\alpha\omega$  is a Floquet factor with  $s$  and  $\alpha$  being real numbers. If the real part of the Floquet factor  $s$  is positive the system will evaluate to a primary instability. Otherwise, the free surface will remain flat and stationary. The  $\alpha$  can take values in the region  $[0, \frac{1}{2}]$ , where  $\alpha=0$  and  $\frac{1}{2}$  correspond to the harmonic and subharmonic responses with respect to the fundamental frequency  $\omega/2\pi$ , respectively. The reality conditions for  $w(z, t)$  and  $\xi(t)$  imply that

$$w_{-n}(z) = w_n^*(z), \quad \xi_{-n} = \xi_n^* \quad (\text{for } \alpha=0), \quad (12)$$

$$w_{-n}(z) = w_n^*(z), \quad \xi_{-n} = \xi_n^* \quad (\text{for } \alpha=\frac{1}{2}). \quad (13)$$

The general solution of Eq. (4) can be written as a linear combination of  $e^{kh}, e^{-kh}, e^{q_n h}, e^{-q_n h}$  with a complex wave number

$$q_n = \sqrt{k^2 + \frac{s+i(\alpha+n)\omega}{\nu}}. \quad (14)$$

Substituting Eqs. (10) and (11) into Eqs. (4)–(9), we can obtain a set of linear homogenous equations of  $\xi_n$ ,

$$\sum_{l=n-N}^{l=n+N} (\mathcal{M}_{n,l} + \mathcal{N}_{n,l}) \xi_n = 0 \quad (n=0, \pm 1, \pm 2, \dots), \quad (15)$$

where

$$\mathcal{M}_{n,l} = \delta_{n,l} \left( g + \frac{\sigma}{\rho}k^2 + \frac{\nu[b_n + c_n \sinh(q_n h) \sinh(kh) + d_n \cosh(q_n h) \cosh(kh)]}{k^2 \sinh(q_n h) \cosh(kh) - k q_n \cosh(q_n h) \sinh(kh)} \right), \quad (16)$$

$$\mathcal{N}_{n,l} = -\frac{1}{2} a_{n-l} e^{i\phi_{n-l}}, \quad (17)$$

$$b_n = 4q_n k^2 (q_n^2 + k^2), \quad (18)$$

$$c_n = k(q_n^4 + 6q_n^2 k^2 + k^4), \quad (19)$$

$$d_n = -q_n(q_n^4 + 2q_n^2 k^2 + 5k^4). \quad (20)$$

The solvable condition of Eq. (15) is

$$\det(\mathcal{M} + \mathcal{N}) = 0. \quad (21)$$

Usually for given geometrical and physical parameters of the fluid layer as well as those of the excitation, a numeric calculation of Eq. (21) can show whether the system is unstable ( $s > 0$ ) or stable ( $s < 0$ ). Furthermore, it can distinguish the primary instabilities between the harmonic ( $\alpha=0$ ) and subharmonic ( $\alpha=\frac{1}{2}$ ) responses as  $s > 0$ . It is necessary in the computation that the matrix with the infinite order is truncated at the order of  $N_{trun}$  according to a given precision. For the MIC, however, the scheme developed by Kumar and Tuckerman [13] is more convenient than that used in the usual instability analysis. Let

$$a_j = a r_j \quad (j=1, \dots, N). \quad (22)$$

We set  $s=0$  and compute the MICs of the harmonic response  $a^H = a^H(k)$  ( $\alpha=0$ ) and the subharmonic one  $a^S = a^S(k)$  ( $\alpha=\frac{1}{2}$ ) satisfying Eq. (21) for other known parameters. The filled circles in Fig. 1 show an example of the MIC of a glycerine-water mixture under the excitation of a square wave with fundamental frequency  $60/2\pi$  Hz, where  $N_{trun}=10$ ,  $N=7$ , and other parameters are the same as Ref. [12]. In the tongue-like zones in Fig. 1, the solutions of the linear instability problem (4)–(9) are unstable, i.e.,  $s > 0$ . The minimum value of  $a$  corresponds to the critical acceleration amplitude  $a_c$ . When  $a < a_c$  the system will keep from the instability and remain flat and stationary. For our example  $a_c = a_c^S = 104.6$  m/s<sup>2</sup> and the onset of instability is in the subharmonic response with respect to the fundamental frequency. In order to compare with those under a single-frequency forcing Fig. 1 (crosses) also shows the tongue-like MICs induced by a sinusoidal wave with a same amplitude. We can see in Fig. 1 that the square wave can induce the instability more effectively than the equal amplitude sinusoidal wave. The period bicriticality, of course, will arise

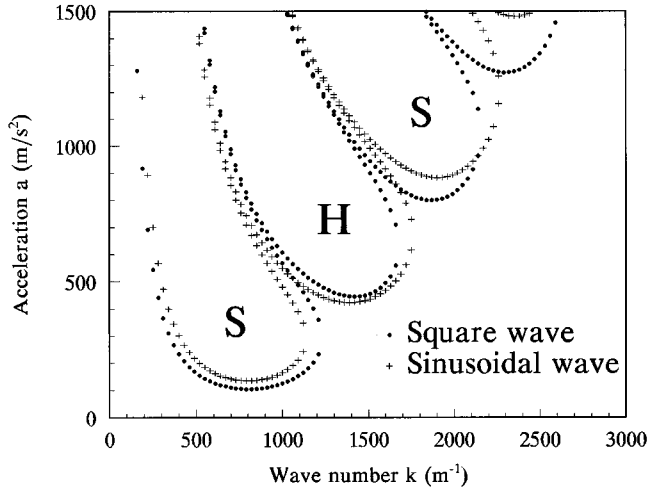


FIG. 1. Primary Faraday instability regions under excitations of a square wave (filled circles) and a sinusoidal wave (crosses).  $H$  and  $S$  denote the instabilities of harmonic and subharmonic responses with respect to the fundamental frequency  $\omega/2\pi$ , respectively. The lowest acceleration amplitude is located at the first subharmonic response tongue under the square wave forcing. The parameters are  $\rho=1220$  kg/m<sup>3</sup>,  $\nu=1.02\times 10^{-4}$  m<sup>2</sup>/s,  $\sigma=6.76\times 10^{-2}$  N/m,  $h=2.0\times 10^{-3}$  m, and  $\omega/2\pi=60$  Hz.

when two minima of acceleration amplitudes  $a_c^S$  and  $a_c^H$  become equal to each other for some suitable parameters.

### III. COMPARISON WITH EXPERIMENTS

As mentioned above, Müller [5] has experimentally observed square and triangular patterns on the surface of a fluid layer under the two-frequency excitation

$$a(t) = a[r\cos(\omega t) + (1-r)\cos(2\omega t + \phi)]. \quad (23)$$

He showed some significant marginal curves including the BTC separating the harmonic and subharmonic region in the plane  $r-\phi$ . Taking  $r_1=r$ ,  $r_2=1-r$ ,  $\phi_1=0$ , and  $\phi_2=\phi$  and setting  $s=0$ , we can obtain the BTC theoretically,

$$r = r(\phi), \quad (24)$$

satisfying

$$a_c^H(r, \phi) = a_c^S(r, \phi). \quad (25)$$

The dotted line in Fig. 2 shows the theoretical BTC of Eq. (24). Comparing with the experimental one (solid curve) [5], although the theoretical BTC is about 21% higher than the experimental one, the result still agrees with the experiments qualitatively. The former, of course, can be reduced by varying the physical parameters, such as by decreasing the surface tension  $\sigma$  and/or the kinetic viscosity  $\nu$ . The dashed line in Fig. 2, which fitted the experimental curve quite well, is a result of decreasing  $\sigma$  to  $1.1\times 10^{-2}$  N/m only. On the other hand, we have to point out that the parameters we used are only the marked values at the temperature 25 °C instead of the real ones at 23 °C at which the experimental BTC was measured. Therefore, we believe that the theory can explain well the experimental BTC if all real values of parameters are known.

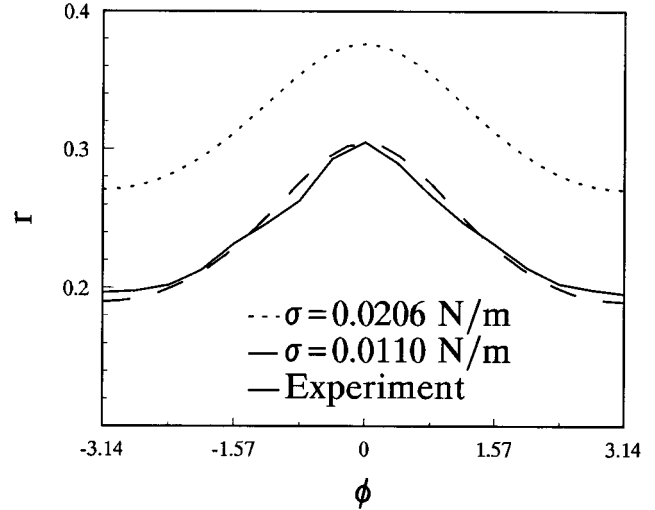


FIG. 2. Bicriticality threshold curves separating the harmonic from the subharmonic region. The solid line is experimental bicriticality threshold curve [5]. The dotted and dashed lines denote the theoretical results with the surface tensions  $\sigma=2.06\times 10^{-2}$  N/m and  $1.1\times 10^{-2}$  N/m, respectively. The other parameters are  $\rho=950$  kg/m<sup>3</sup>,  $\nu=2.0\times 10^{-5}$  m<sup>2</sup>/s,  $h=2.3\times 10^{-3}$  m, and  $\omega/2\pi=27.9$  Hz.

In Müller's experiment, the harmonic response with the fundamental  $\omega/2\pi$  is just the subharmonic response of the second component of the excitation, namely,  $2\omega/2\pi$ , because two components are commensurable with a factor 2. Hence the harmonic response patterns can arise on the surface more easily than the subharmonic patterns can. Edwards and Fauve [6], however, have investigated patterns under the excitations of two incommensurable frequencies

$$a(t) = a[\cos(\chi)\cos(m\omega t) + \sin(\chi)\cos(n\omega t + \phi)], \quad (26)$$

with  $m$  and  $n$  being two incommensurable integers. The patterns and quasipatterns were observed for several sets of  $\{m, n\}$ . In particular, for  $\{4, 5\}$  they completed a systematic investigation and measured the MICs for  $\phi=75^\circ$  in the polar plane of parameters  $a$  and  $\chi$  (see the solid lines in Fig. 12 of Ref. [6]). Although Eq. (26) is no longer a periodic function with period  $2\pi/m\omega$  ( $m < n$  assumed), it is still a periodic function of time with a fundamental period  $2\pi/\omega$ . According to the experimental conditions we set  $N_{run}=10$ ,  $N=5$ ,  $s=0$ , and forcing parameters

$$r_1=r_2=r_3=0, \quad r_4=\cos(\chi), \quad r_5=\sin(\chi),$$

$$\phi_1=\phi_2=\phi_3=\phi_4=0, \quad \phi_5=75^\circ \quad (27)$$

and all physical and geometrical parameters are the same as those in Ref. [6]. For every value of  $\chi$  the minima of  $a_c^H$  and  $a_c^S$  can be picked out from the solutions of Eq. (21) for  $\alpha=0$  and  $\frac{1}{2}$ , respectively. The numerical results have been plotted by filled circles and diamonds in Fig. 3, where the former correspond to the harmonic response and the latter to the subharmonic. Although there is no any adjustable parameter in the computation, the result still agrees well with the experiments quantitatively. It is easy to see in Fig. 3 that this stability region is enclosed with two MICs and that there is a

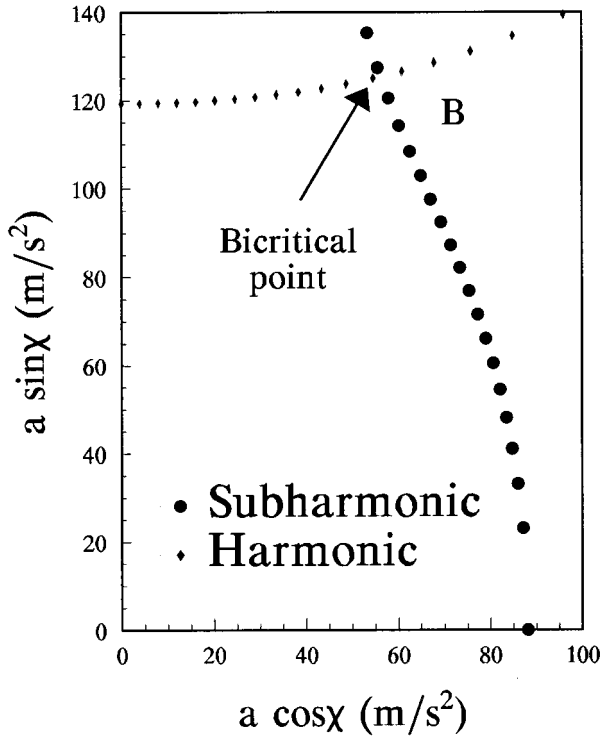


FIG. 3. Marginal instability curves for  $\phi=75^\circ$  in the polar plane of  $a$  and  $\chi$ . The filled circles and filled diamonds separate the stability region from the harmonic and subharmonic instability regions, respectively. The intersection of two curves is a bicriticality point. All parameters are the same as those in Ref. [6], namely,  $\rho=1220 \text{ kg/m}^3$ ,  $\nu=1.0\times 10^{-4} \text{ m}^2/\text{s}$ ,  $\sigma=6.5\times 10^{-2} \text{ N/m}$ ,  $h=2.9\times 10^{-3} \text{ m}$ , and  $\omega/2\pi=14.6 \text{ Hz}$ .

period bicriticality point  $B$  at the intersection of two MICs at which Edwards and Fauve found a different phenomenon: a 12-fold quasipattern. The experimental measurement discovered that the wave number of patterns will be about  $8.8 \text{ cm}^{-1}$  for  $\chi > \chi_B$  ( $\chi$  at point  $B$ ) and about  $7.4 \text{ cm}^{-1}$  for  $\chi < \chi_B$ . Obviously, for large  $\chi > \chi_B$ , the excitation is mainly from the frequency component  $5\omega/2\pi$  and the patterns will respond with its subharmonic  $\frac{5}{2}\omega/2\pi$ , which is a subharmonic of the fundamental  $\omega/2\pi$ . Otherwise, the patterns will respond with the subharmonic of  $4\omega/2\pi$ , namely,  $\frac{4}{2}\omega/2\pi$ , which is a harmonic of the fundamental  $\omega/2\pi$ . It is obvious that the bicriticality point of the wave number is just that of the wave period at which the competition between harmonic

and subharmonic responses takes place. Therefore, the calculation can explain well the corresponding observations.

#### IV. CONCLUSION

The linear instability analysis developed by Kumar [12] has been extended to the Faraday pattern experiments under an arbitrarily periodic excitation. Using this extended linear instability analysis, one can easily analyze the primary instabilities for various Faraday experiments, such as those under the excitations of a square wave, a triangle wave, and any multiple-frequency wave. As an interesting application we have analyzed the primary Faraday instabilities under the excitations of two frequencies. Comparing with the known experiments, the theoretical results show clearly both the BTC, which separates the harmonic and subharmonic responses [5], and the MIC which separates the primary pattern and the flat surface [6] in the plane of exciting parameters. Although the matrix in Eq. (21) has to be truncated approximately in a detailed calculation, a good convergence of the theory allows one to neglect the difference due to the truncation for an  $N_{run}$  slightly larger than the frequency truncation  $N$ . Furthermore, the critical instability under an arbitrarily periodic excitation with any preassigned accuracy can be determined by increasing the truncation number. The multiple-frequency Faraday experiment has been understood as an opportunity to investigate the interaction between two modes of the pattern [6]. The extended theory here can determine the central region (or point) in which the interaction arises. Furthermore, the extended theory can also investigate the multiple criticality at which there will be a quasipattern with the competition among the multiple periods (wave numbers) in the multiple-frequency Faraday experiment. Therefore, it is important to further understand the mechanism of the pattern formation in the Faraday experiment. We are now in the process of an experiment together with a systematic computation for the observation of the multiple criticality. The extended theory, of course, can be also further generalized to the interface system of two fluids [13,15].

#### ACKNOWLEDGMENTS

The authors would like to thank Professor Benren Wang and Professor Guoqing Miao of Nanjing University for their helpful discussions. This work was supported by the Scaling Plan of the People's Republic of China and the Natural Science Foundation of Zhejiang Province, People's Republic of China.

- 
- [1] M. Faraday, Philos. Trans. R. Soc. London **52**, 319 (1831).
  - [2] W. S. Edwards and S. Fauve, Phys. Rev. E **47**, R788 (1993).
  - [3] K. Kumar and K. M. S. Bajaj, Phys. Rev. E **52**, R4606 (1995).
  - [4] D. Binks and W. van de Water, Phys. Rev. Lett. **78**, 4043 (1997).
  - [5] H. W. Müller, Phys. Rev. Lett. **71**, 3287 (1993).
  - [6] W. S. Edwards and S. Fauve, J. Fluid Mech. **278**, 123 (1994).
  - [7] J. R. Wu, R. Keolian, and I. Rudnick, Phys. Rev. Lett. **52**, 1421 (1984).
  - [8] W. Z. Chen, R. J. Wei, and B. R. Wang, Phys. Rev. E **53**, 6016 (1996).
  - [9] W. B. Zhang and J. Vinal, Phys. Rev. Lett. **74**, 690 (1995).
  - [10] A. Kudrolli and J. P. Gollub, Phys. Rev. E **54**, R1052 (1996).
  - [11] T. B. Benjamin and F. Ursell, Proc. R. Soc. London, Ser. A **225**, 505 (1954).
  - [12] K. Kumar, Proc. R. Soc. London, Ser. A **452**, 1113 (1996).
  - [13] K. Kumar and L. S. Tuckerman, J. Fluid Mech. **279**, 49 (1994).
  - [14] H. W. Müller, H. Wittmer, C. Wanger, and K. Knorr, Phys. Rev. Lett. **78**, 2357 (1997).
  - [15] W. Z. Chen, R. J. Wei, and B. R. Wang, Phys. Lett. A **208**, 197 (1995).